

A Low-Power Multi-Phase Oscillator with Transfer Gate Phase Coupler Enabling Even-Numbered Phase Output

Toshihiro KONISHI^{†a)}, Student Member, Hyeokjong LEE[†], Nonmember, Shintaro IZUMI[†], Student Member, Takashi TAKEUCHI[†], Nonmember, Masahiko YOSHIMOTO[†], and Hiroshi KAWAGUCHI[†], Members

SUMMARY We propose a transfer gate phase coupler for a low-power multi-phase oscillator (MPOSC). The phase coupler is an nMOS transfer gate, which does not waste charge to the ground and thus achieves low power. The proposed MPOSC can set the number of outputs to an arbitrary number. The test circuit in a 180-nm process and a 65-nm process exhibits 20 phases, including 90° different angles. The designs in a 180-nm CMOS process and a 65-nm CMOS process were fabricated to confirm its process scalability; in the respective designs, we observed 36.6% and 38.3% improvements in a power-delay products, compared with the conventional MPOSCs using inverters and nMOS latches. In a 65-nm process, the measured DNL and 3 σ period jitter are, respectively, less than $\pm 1.22^\circ$ and 5.82 ps. The power is 284 μ W at 1.85 GHz.

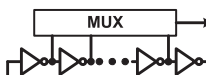
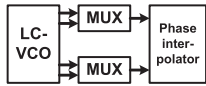
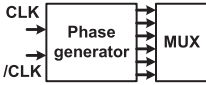
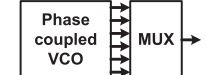
key words: multi-phase oscillator, transfer gate phase coupler, even-numbered phases, low-power, process scalable

1. Introduction

Ring oscillators, which output multiple phases, are widely used in signal processing. Particularly, multiple phases with a small clock skew ring oscillators are used: the high-resolution phases enable writing to optical disks [1]–[5]. A serial link receiver for a compact disk recordable (CD-R) requires a multi-phase generator and a number of phase rotators to produce data and edge clocks.

There are four methods for generating multiple phases as shown in Table 1. First, a ring oscillator consists of multiple-stage inverters. This method is very simple, but it cannot generate multiple phases at high frequency [4]. Second, multiple phases can be generated by an inductor-capacitor voltage controlled oscillator (LC-VCO) with phase interpolator. This has lower-power consumption and higher resolution than the ring oscillator. Unfortunately, it has a narrow-band frequency due to inductor's high quality factor (Q). The third phase generator is based on a poly-phase filter. This method has lower power and lower cost than other methods. However, it needs external clocks [5]. The other way is a multi-phase oscillator (MPOSC) that uses phase coupled inverter chains [1]–[3], [6], [7]. High frequency with wide-band output can be achieved using the MPOSC. However, the conventional inverter-structured and latch-structured phase couplers draw the charge to the ground, meaning that the phase couplers

Table 1 Comparison of multi-phase oscillators and other circuits generating multiple phases.

Type	Circuit Configuration	Characteristics
A set of inverter chain		Coarse phase resolution Large power Large size inverter needed
Quadrature LC-VCO & phase interpolator		Middle phase resolution Low power Narrow frequency band
External clocks & poly-phase filter		Fine phase resolution Small area and low power External clock needed
Phase coupled VCO		Fine phase resolution Middle power Wide frequency band

consume unnecessary power themselves [1], [2], [6]. There is another option like a resistance element as a phase coupler [8]: Resistor, nMOS transistor, pMOS transistor, or CMOS switch. However, it draws static current in a locked state and thus consumes needless power. To make matters worse, the transistor-type couplers require an external analog input voltage.

In this paper, we propose to adopt a transfer gate phase coupler (TGPC) that wastes no charge to the ground, which enables a low-power MPOSC; it fully achieves the benefits from process scaling. We also explain the charge operation of the TGPC. By using the TGPC, we can set the number of inverter chains to an even number. It is confirmed that the TGPC possesses process scalability with implementations in 180-nm and 65-nm processes.

This paper is organized as follows: Sect. 2 describes phase couplers in the conventional and proposed low-power MPOSC. Careful design for layout is mentioned in Sect. 3. Section 4 states measurement results in 180-nm and 65-nm test chips. The final section concludes this paper.

2. Phase Coupler Design

2.1 Relation between Oscillation and Phase in MPOSC

The period of a ring oscillator, T , is determined by a delay of inverter:

$$2n \times \text{delay} = T \quad (1)$$

Manuscript received March 26, 2011.

Manuscript revised June 22, 2011.

[†]The authors are with the Department of Computer Science and Systems Engineering, Kobe University, Kobe-shi, 657-8501 Japan.

a) E-mail: air@cs28.cs.kobe-u.ac.jp

DOI: 10.1587/transfun.E94.A.2701

where n is the number of stages in the ring oscillator, and it must be a odd number, thus three or more. On the other hand, as for a phase resolution, θ_{res} , it signifies a phase difference between an input and output of the two inverters, and it is defined as $360^\circ/n$. The oscillating frequency and phase resolution depend on only the number of inverter stages. For a higher oscillating frequency, large-sized inverters are necessitated, resulting in larger power.

The MPOSC can consist of coupled inverter chains. In other words, the frequency and the phases are defined respectively by inverter chains and phase couplers. Those are made to one eventual ring, where phase couplers are link to inverter chains [2].

The phase coupled MPOSC obtains $n \times m$ phases from m sets of n -stage ring oscillators. It can be, therefore, considered as one set of $n \times m$ -stage ring oscillator: θ_{res} becomes $360^\circ/(n \times m)$.

2.2 Phase Couplers in Conventional MPOSC

The conventional current-controlled MPOSC is shown in Fig. 1, with two kinds of phase couplers. The inverter-structured phase coupler in Fig. 1(b) does a full swing of charge between inverter chains. For this reason, oscillation frequency depends on not only inverter chains but also the ring of phase couplers. Thus, when making many phases, the ring of the phase coupler delays larger, which limits oscillating frequency.

Another conventional approach is a latch-structured phase coupler shown in Fig. 1(c). The latch of two nMOS makes a half swing of charge between inverter chains. Although the phase couplers have certain relation, it does not give an impact like the inverter coupler. The oscillating frequency depends on only inverter chains, and it can oscillate at higher frequency [2].

In this way, the conventional MPOSCs consume power

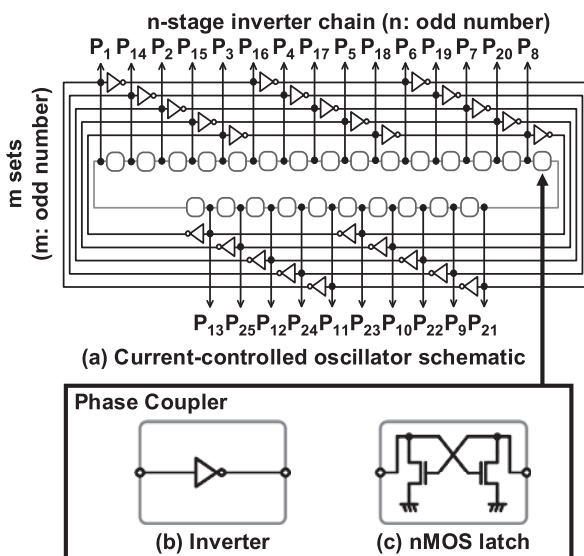


Fig. 1 Conventional MPOSC schemes.

for the swing of charge by the phase couplers between the inverter chains. When nMOS of the inverter-structured phase coupler is turned on, it discharges through the inverter. The latch-structured phase coupler does so. The conventional phase coupler draws current to the ground through itself and consumes power even if the MPOSC is locked. Thereby, the conventional MPOSC wastes more power than the ring oscillator composed of the same number of stages.

We explain the 5×5 MPOSC with the inverter phase coupler (Fig. 1) in detail using Fig. 2. As for this MPOSC, P_1 is connected to the input of the phase coupler PC_1 , and its output P_{14} is connected to the output of the inverter INV_1 . Additionally, P_{14} is connected to the input of the PC_2 . The nMOS or pMOS of the phase coupler becomes active by the P_1 state. When the nMOS becomes active, P_{14} is discharged. On the other hand, when the pMOS becomes active, P_{14} is charged. When P_{14} was delayed, it is discharged by the nMOS of phase coupler (on the rising edge, P_{14} will be charged after the pMOS becomes active). In contrast, when P_{14} was advanced, it is locked for the same reason.

The other conventional approach using the latch as a phase coupler is explained in Fig. 3. P_1 and P_{14} are cross-coupled by the latch. When P_1 is “high”, the P_{14} ’s charge flows to the ground; On the other hand, if P_{14} is “high”, the P_1 ’s charge flows to the ground. As a result, P_1 and P_{14} try to be stable as they have inverse phases each other, which is the basis of the latch-structured phase coupler, similar to the inverter phase coupler’s case. Note that the phase coupling operation is carried out only when P_1 is “high” and active (This is the reason why the latch-structured phase coupler does “the half-swing of charge”) Then, P_{14} cross-coupled with P_2 is processed in the same way. Consequently, P_{14} is locked to the opposite phase of the middle phase between P_1 and P_2 .

2.3 Proposed Transfer Gate Phase Coupler

Now, m sets of n -stage ring oscillators in Fig. 1 are considered. Because the inverter or latch in Fig. 1(b) or 1(c) is used

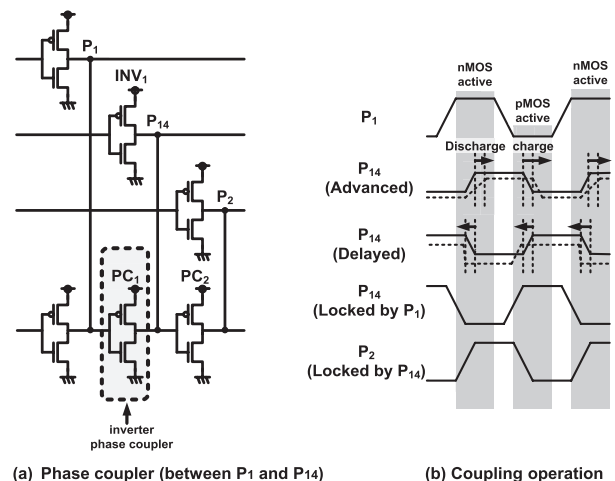


Fig. 2 Principle of inverter phase coupler.

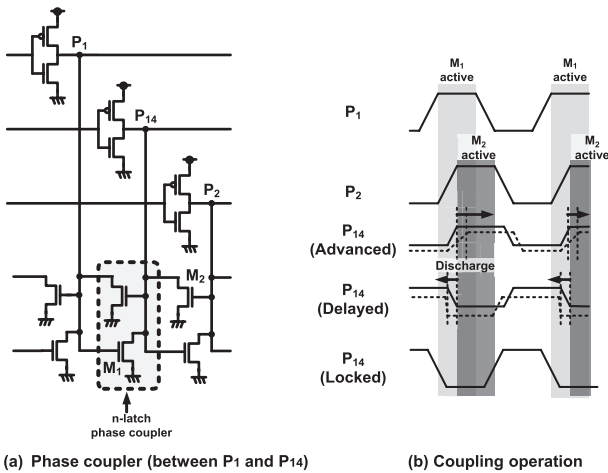


Fig. 3 Principle of latch phase coupler.

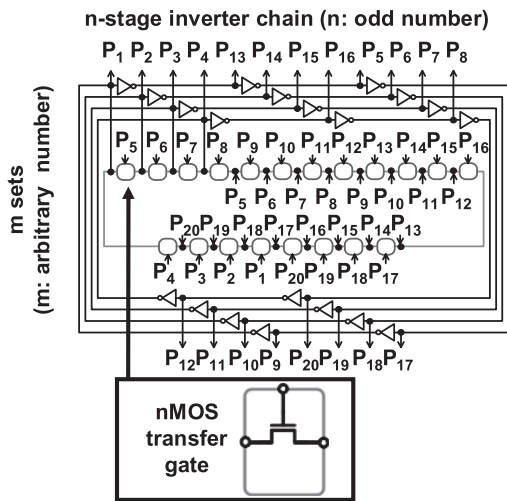


Fig. 4 Proposed MPOSC scheme.

as a phase coupler in the conventional MPOSC, it inverts a phase signal, which means that m must be an odd number; otherwise, the ring is stabilized and is not oscillated. In contrast, our MPOSC scheme adopts the nMOS transfer gate presented in Fig. 4; it does not accompany the inverting operation as a phase coupler. Consequently, the proposed scheme can accommodate setting of m to an arbitrary number; we can thus set m to an even number in the proposed scheme, which enables even-numbered phase outputs.

For instance, the minimal components that create I/Q signals (90° differential signal) are $m = 4$ and $n = 3$ in our MPOSC. The phases in this type of MPOSC is shown in Fig. 5. In the practical design, we chose $m = 4$ and $n = 5$ ($\theta_{res} = 18^\circ$) by increasing the number of stages in the inverter chain for finer phase resolution and lower jitter. A 72° delayed signal is used to turn on an nMOS TGPC. A detailed schematic of our proposed design is presented in Fig. 6.

The proposed TGPC uses an nMOS controlled by the outputs of the inverter chains. The waveforms of the pro-

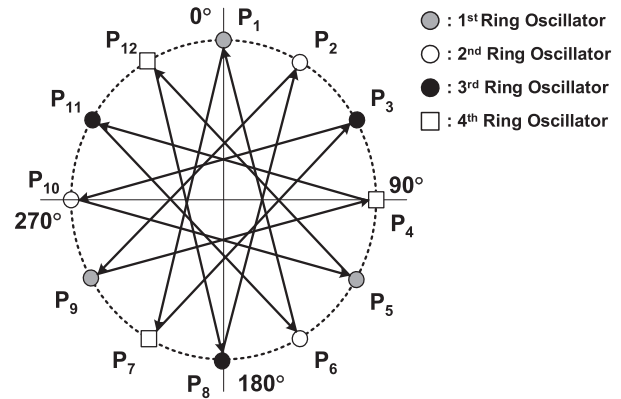


Fig. 5 Phases in the proposed 4×3 -stage MPOSC.

posed TGPC, which further explain the operation principle, are portrayed in Fig. 7. In fact, P_4 and P_8 are derived from the same ring oscillator as shown in Fig. 4. Their mutual phase relation is stable 72° , and P_8 controls the phase coupler connected with P_4 . Because of the stable 72° delay of P_8 behind P_4 , P_8 can always turn on the nMOS TGPC at the P_4 's falling edge. The TGPC equalizes P_3 and P_4 , and also P_4 and P_5 if they are not locked. Depending on the both voltages at the TGPC's drain and source, the time to be locked will vary.

For a case in which P_4 is delayed behind P_3 , the current from P_4 is drawn through TGPC M_1 to P_3 , by which the P_4 's falling edge becomes advanced. In contrast, if P_4 is advanced, P_4 is delayed by P_5 . For these reasons, P_4 is locked to the middle phase between P_3 and P_5 . The TGPC using P_3 , P_5 , P_8 and P_9 can determine the P_4 's phase. Once P_3 , P_4 and P_5 are locked, the current flows less because the voltage difference between them is quite small. The current is decreased with the increase of a phase number because the different voltage becomes smaller. Consequently, our proposed MPOSC is highly effective for developing the oscillation; the TGPC's power overhead can be minimized.

3. Layout Design

Because the goal of MPOSC is to align phase outputs, the layout of the MPOSC must be carefully designed for high phase resolution. A differential nonlinearity (DNL), which represents a phase error between the nearest two phases, is affected by loads of outputs, parasitic resistance and capacitance (RC) derived from wires and vias, and peripheral circuits. For this reason, a detailed RC extract from layout and circuits simulation using it have to be conducted in an MPOSC. In particular, in the proposed MPOSC, there are more ports with TGPCs, resulting in complicated wiring.

In the proposed MPOSC, the circuits can be divided into two blocks: One block includes inverters, and the other is a block comprising of TGPCs. The phase outputs from the inverter block are input to the TGPC block, in which the inputs are connected to TGPC's gates, drains and sources. We have to consider the layouts of the two circuit blocks,

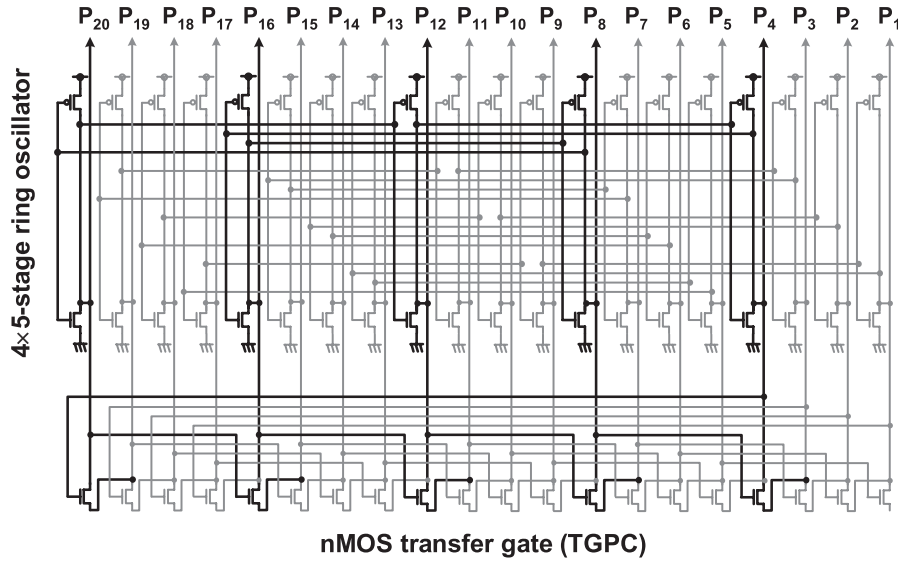


Fig. 6 Detailed schematic of proposed MPOSC.

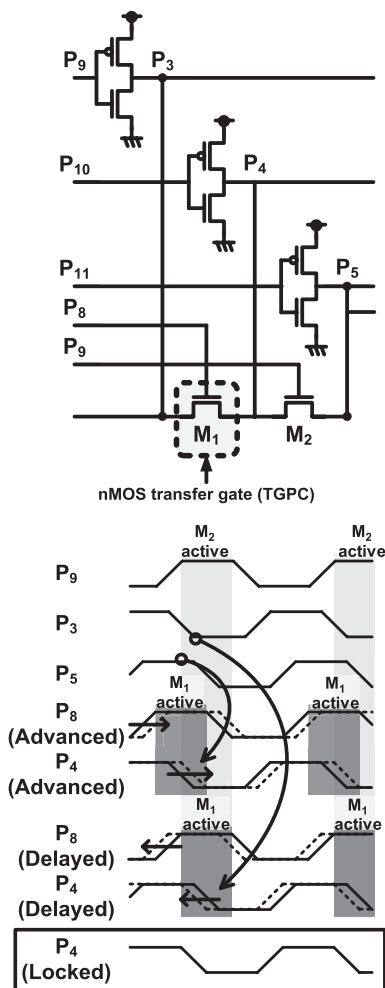


Fig. 7 Principle of the transfer gate phase coupler.

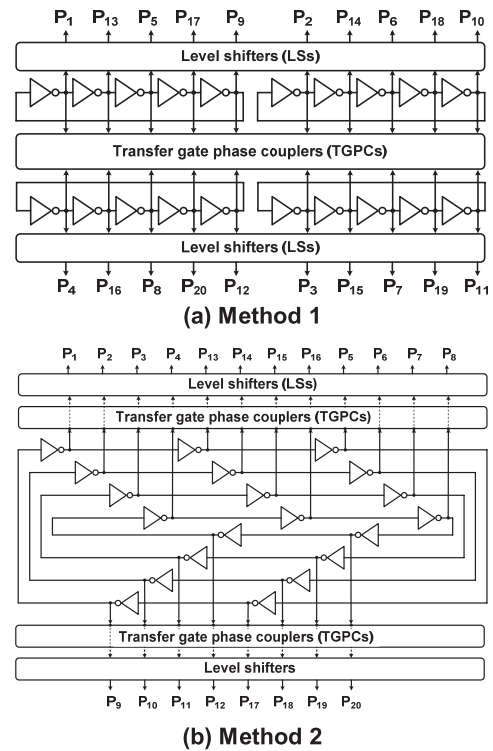


Fig. 8 (a) Method 1: phase coupler centered and (b) Method 2: inverter centered topologies.

and level shifters (LS = output buffers) for external output. We simulated two kinds of circuit topologies shown

in Fig. 8. Method 1 in Fig. 8(a) is a TGPC centered design. Load variation of the inverters' outputs is alleviating by placing the inverter near the LSs. Method 2 is an inverter centered design as shown in Fig. 8(b). We separate the LSs' block from the inverters. The inverter block's outputs and the TGPC block's inputs are located in the same places; thus the parasitic resistance and capacitance, and via resistance can be reduced by simple wiring. The distance between LSs and inverters is, however, long, which delays

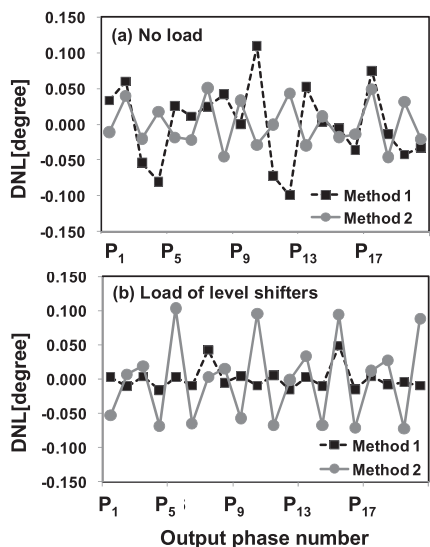


Fig. 9 Simulated DNLs in two layouts.

signal transmission to the LSs.

Figure 9 shows simulation results in the two layout methods: Figs. 9(a) and 9(b) correspond to cases that the inverters have no load and LSs as load, respectively. If no load, Method 2 is better than Method 1 in terms of DNL. The respective DNLs in Methods 1 and 2 are 0.044° and 0.028° on average. This is because the wiring resistance and capacitance, and via resistance to the phase couplers are lower in Method 2. In reality, the Method 2’s oscillating frequency is higher.

In contrast, when an LS is considered as the inverter’s load, the oscillating frequencies are lowered by 20.4% in the both methods. The DNLs exhibit different results from the case of no load: The average DNL in Method 1 is decreased to 0.012° from 0.044° in the no-load case, whereas that in Method 2 is increased from 0.028° to 0.051° . This is because the wiring distance between the inverter and LS are adversely affected. The LSs are prepared for driving external circuits and are also connected to source followers to measure waveforms. This gives affects to the load of the inverters, which may cause variation to the DNL performance. Consequently, we chose Method 1 as the MPOSC layout.

4. VLSI Implementation and Measurement Results

We implemented the proposed MPOSC in a 180-nm and 65-nm process technologies, using the layout described in the previous section.

4.1 180-nm Test Chip

Figure 10(a) portrays a test chip of the proposed MPOSC core with the 180-nm CMOS process technology. The output from the four sets of five-stage ring oscillators is 20 phases, including I/Q signals. The core layout is shown in Fig. 10(b), and its area is $40.6 \times 54.2 \mu\text{m}^2$, including the LSs

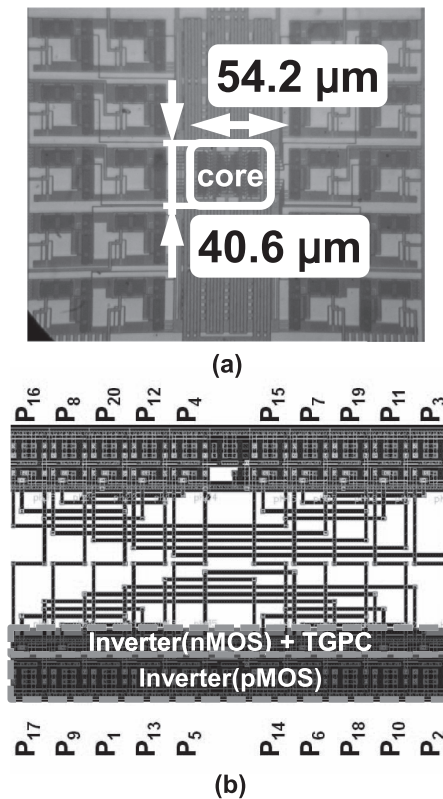


Fig. 10 (a) Photograph of 180-nm test chip and (b) its core layout.

that drive the external source followers. At a supply voltage of 1.5 V, our designed MPOSC outputs 433 MHz that complies with ISO/IEC 18000-7.

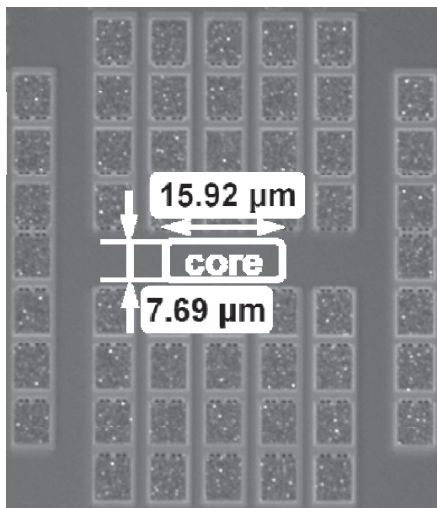
4.2 65-nm Test Chip

Figure 11(a) portrays a test chip layout in a 65-nm CMOS process technology. The structure is the same as the above. The core layout is shown in Fig. 11(b), and its area is $15.92 \times 7.69 \mu\text{m}^2$, including the LSs that drive the external source followers. This result shows that the proposed MPOSC has process scalability and that its chip area can be reduced through process scaling.

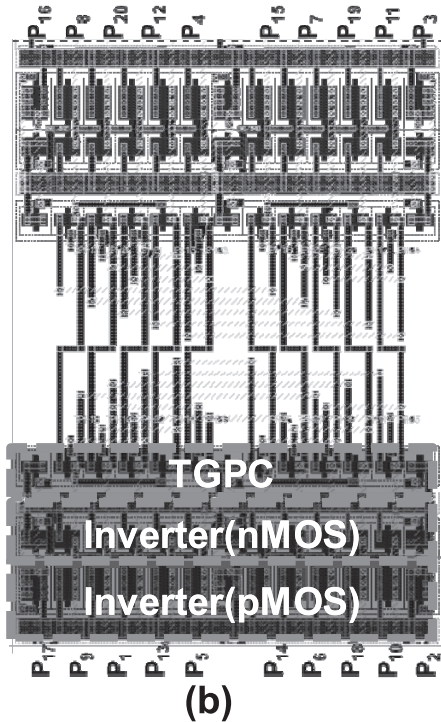
4.3 Performances

The result measurements of the 180-nm and 65-nm CMOS process technologies are shown in Table 2. We confirmed that the oscillating frequencies in the 180-nm and 65-nm processes respectively achieve 581 MHz at a supply voltage of 1.8 V and 1.85 GHz at a supply voltage of 1.2 V. The measured 3σ period jitter in the 180-nm node is 12.0 ps at 581 MHz, and that in the 65-nm node is 5.82 ps at 1.85 GHz. Figures 12 and 13 shows waveforms from source followers as measured examples (P_3 and P_4 : 18° different).

Figure 14 shows the DNL measured at the same frequency. The maximum DNL is less than $\pm 1.50^\circ$ in the 180-nm CMOS process. In the 65-nm CMOS process, the maximum DNL is less than $\pm 1.22^\circ$.



(a)

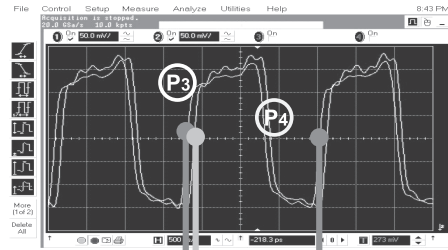


(b)

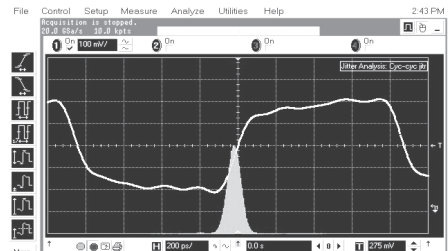
Fig. 11 (a) Photograph of 65-nm test chip and (b) its core layout.

Table 2 The proposed MPOSC measurement result.

	[2]	This work	This work
Process	65-nm CMOS	180-nm CMOS	65-nm CMOS
Output frequency	24.8–490MHz	120–581 MHz	0.024–1.85 GHz
Phase resolution	T/63 (>32ps)	T/20 (>86 ps)	T/20 (>27 ps)
DNL of output phase	-1.0 to 0.8LSB @ 490 MHz	-1.30 to 1.50deg. @ 581 MHz	-1.22 to 0.86deg. @ 1.85 GHz
Period jitter (3σ)	3.47ps@490MHz	12.0 ps @ 581 MHz	5.82 ps @ 1.85 GHz
Accumulation jitter (3σ)	13.7ps@490MHz (3000 clocks)	26.3 ps(100 clocks)	12.8 ps(100 clocks)
Power consumption	N/A	920 μW @ 581 MHz	284μW @ 1.85 GHz
Core size	36 μm × 46 μm	54.2 μm × 40.6 μm	15.92 μm × 7.69 μm

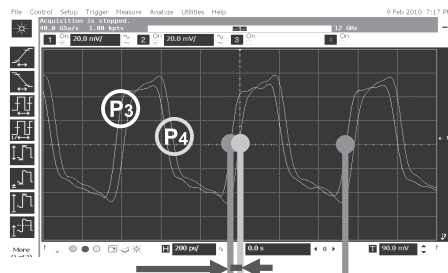


(a) Phase outputs: P₃ and P₄

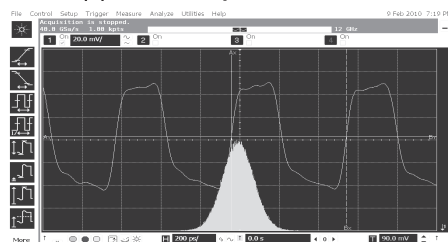


Standard deviation (std dev) : 3.9887 ps
3σ period jitter = std dev × 3 = 12.0 ps
(b) Period jitter

Fig. 12 Measured waveforms and period jitter in 180-nm process.



(a) Phase outputs: P₃ and P₄



Standard deviation : 1.93807 ps
3σ period jitter = std dev × 3 = 5.81 ps
(b) Period jitter

Fig. 13 Measured waveforms and period jitter in 65-nm process.

In the 180-nm CMOS process, a comparison of the power-delay (PD) products between the conventional MPOSCs and the proposed MPOSC is depicted in Fig. 15. The structures of the oscillators in the figure are the simple 1-set ring oscillator (Ring OSC) and the MPOSCs using the inverter type phase couplers (Inverter [1]), the nMOS latch type ones (nMOS latch [2]), and the proposed TGPC. Note that the MPOSCs consist of a same set number and a same

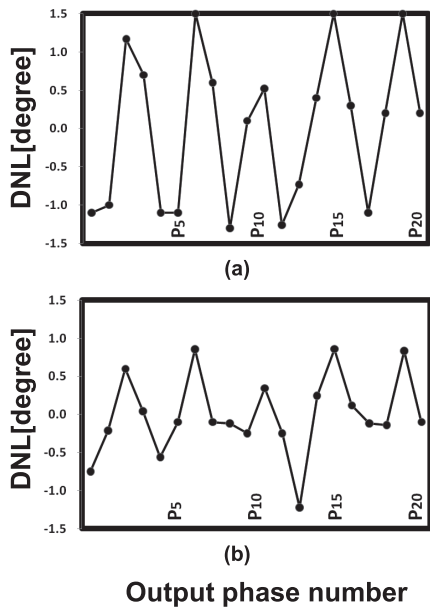


Fig. 14 Measured DNLs in (a) 180-nm and (b) 65-nm processes.

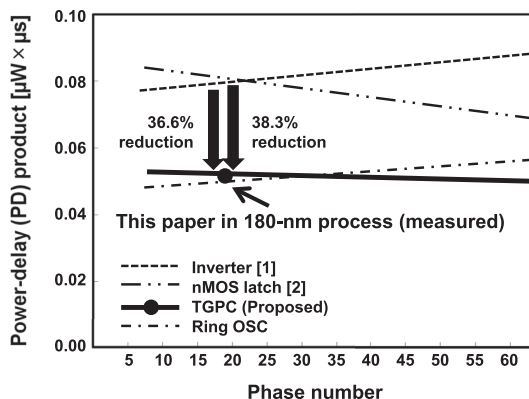


Fig. 15 Comparison of PD products of MPOSCs and ring oscillator.

stage number from 3×3 stages to 9×7 stages but the types of the phase couplers are merely different, and the simple 1-set ring oscillator has the same number of inverters. The results show that the proposed MPOSC with the TGPCs is superior to the other MPOSCs. As the phase number increase, it becomes more effective in power. It is comparable to the ring oscillator that does not use phase coupling. We observed that 36.6% and 38.3% improvements can be achieved, respectively, compared with the conventional MPOSCs with the inverters and nMOS latches. The PD products of the simple ring oscillator will be higher than the MPOSC with the TGPCs, at a phase number of 35 and more. This is because, in the simple ring oscillator, the oscillating frequency is decreased with increasing the number of phases and the number of inverters. To obtain a higher oscillating frequency and a greater number of phases, large-sized inverters are necessitated, which results in larger power dissipation.

Figure 16 confirmed the process scalability of the 180-

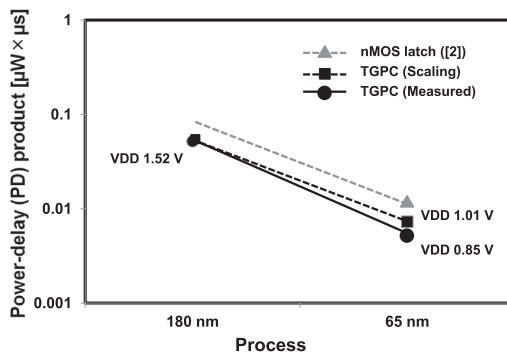


Fig. 16 Shift of PD products with process scaling.

nm CMOS process and the 65-nm CMOS process. The PD product when setting oscillation frequency to 450 MHz is measured. It is understood that the proposed TGPC oscillator is superior to the conventional MPOSC in low-power consumption. In particular, when the same frequency is set in each process, the supply voltage can be lower by scaling. As a result, we confirmed that the PD product can be made lower than that in the conventional one by this measure.

5. Conclusion

In this paper, we propose a low-power MPOSC with single-end inverters and the TGPCs. It can set the number of inverter chains to an arbitrary number. The proposed architecture is simply implemented by transistors, and does not use any analog elements. So, the architecture can benefit from process scaling. We have implemented the proposed MPOSCs in a 180-nm CMOS process and a 65-nm CMOS process, which respectively consumed power of $920 \mu\text{W}$ at 581 MHz and $284 \mu\text{W}$ at 1.85 GHz, indicating that our proposed MPOSC is suitable for process scaling.

Acknowledgments

This research was partially supported by the Strategic Information and Communications R&D Promotion Program (SCOPE), the Ministry of Internal Affairs and Communications, Japan. The chip development was performed by STARC, Japan, and the Japanese Ministry of Economy, Trade and Industry sponsored “Silicon Implementation Support Program for Next Generation Semiconductor Circuit Architectures”. This research was also supported by the VLSI Design and Education Center (VDEC) of The University of Tokyo in collaboration with Synopsys Inc., Cadence Design Systems Inc., Mentor Graphics Corp., and Agilent Technologies Japan Ltd.

References

- [1] J.G. Maneatis and M.A. Horowitz, “Precise delay generation using coupled oscillators,” *IEEE J. Solid-State Circuits*, vol.28, no.12, pp.1273–1282, Dec. 1993.
- [2] A. Matsumoto, S. Sakiyama, Y. Tokunaga, T. Morie, and S. Dosho, “A design method and developments of a low-power and high-resolution

multiphase generation system," IEEE J. Solid-State Circuits, vol.43, no.4, pp.831–843, April 2008.

- [3] Y. Konno, K. Tomioka, Y. Aiba, K. Yamazoe, and B.-S. Song, "A CMOS 1×- to 16×- speed DVD write channel IC," IEEE ISSCC Dig. Tech. Papers, pp.568–569, 2005.
- [4] Y.-S. Kim, S.-J. Park, Y.-S. Kim, D.-B. Jang, S.-W. Jeong, H.-J. Park, and J.-Y. Sim, "A 40-to-800 MHz locking multi-phase DLL," IEEE ISSCC Dig. Tech. Papers, pp.306–307, 2007.
- [5] K. Kim, D.M. Dreps, F.D. Ferraiolo, P.W. Coteus, S. Kim, S.V. Rylov, and D.J. Friedman, "A 5.4 mW 0.0035 mm² 0.48 psrms-Jitter 0.8-to-5 GHz non-PLL/DLL all-digital phase generator/rotator in 45 nm SOI CMOS," IEEE ISSCC Dig. Tech. Papers, pp.98–99, 2009.
- [6] E.G. Friedman and S. Powell, "Design and analysis of a hierarchical clock distribution system for synchronous standard cell/macrocell VLSI," IEEE J. Solid-State Circuits, vol.SC-21, no.2, pp.240–246, April 1986.
- [7] L. Sun and T.A. Kwansniewski, "A 1.25-GHz 0.35- μ m monolithic CMOS PLL based on a multiphase ring oscillator," IEEE J. Solid-State Circuits, vol.36, no.6, pp.910–916, June 2001.
- [8] S. Watanabe, T. Oka, and T. Arakawa, "Multi-phase oscillator," U.S. patent 2009/0261911 A1.



Toshihiro Konishi was born on November 13, 1985. He received his B.E. and M.E. degree from Kobe University, Hyogo, Japan in 2008 and 2010, respectively. He is currently on the doctoral course at Kobe University. His research interests include digitally controlled oscillator and low-power A-D converter designs and digital signal processing. He is a member of the IEEE.



Hyeokjong Lee received his B.E. degree in Electrical and Electronic Engineering from Kanazawa University in 2007. He received his M.E. degree in Computer Science and Systems Engineering from Kobe University in 2009. His interests include low power mixed-signal circuits.



Shintaro Izumi respectively received his B.E. and M.E. degrees in Computer Science and Systems Engineering from Kobe University, Hyogo, Japan, in 2007 and 2008. He received his Ph.D. degree in Engineering from Kobe University in 2011. He was a JSPS research fellow at Kobe University from 2009 to 2011. Since 2011, he has been a Assistant Professor in the Organization of Advanced Science and Technology at Kobe University. His current research interests include communication protocols, low-power VLSI design, and sensor networks. He is a member of the IEEE.



Takashi Takeuchi received his B.E. degree in Electrical and Electronic Engineering from Kanazawa University in 2005. He received his M.E. degree in Computer Science and Systems Engineering from Kobe University in 2007. He received his Ph.D. degree in Engineering from Kobe University, Kobe, Japan in 2010. His interests include low-power analog circuit designs.



Masahiko Yoshimoto received his B.S. degree in Electronic Engineering from Nagoya Institute of Technology, Nagoya, Japan, in 1975, and his M.S. degree in Electronic Engineering from Nagoya University, Nagoya, Japan, in 1977. He received his Ph.D. degree in Electrical Engineering from Nagoya University, Nagoya, Japan in 1998. He joined the LSI Laboratory, Mitsubishi Electric Corp., Itami, Japan, in April 1977. From 1978 to 1983 he was engaged in the design of NMOS and CMOS static RAM,

including a 64 K full CMOS RAM with the world's first divided-word-line structure. From 1984, he was involved in research and development of multimedia ULSI systems for digital broadcasting and digital communication systems based on MPEG2 and MPEG4 Codec LSI core technology. Since 2000, he has been a Professor of the Dept. of Electrical and Electronic Systems Engineering at Kanazawa University, Japan. Since 2004, he has been a Professor of the Dept. of Computer and Systems Engineering at Kobe University, Japan. His current activity is focused on research and development of multimedia and ubiquitous media VLSI systems including an ultra-low-power image compression processor and a low power wireless interface circuit. He holds 70 registered patents. He served on the Program Committee of the IEEE International Solid State Circuit Conference from 1991 to 1993. In addition, he has served as a Guest Editor for special issues on Low-Power System LSI, IP, and Related Technologies of IEICE Transactions in 2004. He received the R&D 100 awards from R&D Magazine for development of the DISP and development of a real-time MPEG2 video encoder chipset in 1990 and 1996, respectively.



Hiroshi Kawaguchi received his B.E. and M.E. degrees in Electronic Engineering from Chiba University, Chiba, Japan, in 1991 and 1993, respectively, and his Ph.D. degree in Engineering from the University of Tokyo, Tokyo, Japan, in 2006. He joined Konami Corporation, Kobe, Japan, in 1993, where he developed arcade entertainment systems. He moved to the Institute of Industrial Science, the University of Tokyo, as a Technical Associate in 1996, and was appointed a Research Associate in 2003. In

2005, he moved to Kobe University, Kobe, Japan, and since 2007, he has been an Associate Professor with the Department of Computer Science and Systems Engineering at the same university. He is also a Collaborative Researcher with the Institute of Industrial Science, the University of Tokyo. His current research interests include low-power VLSI design, hardware design for wireless sensor network, and recognition processor. Dr. Kawaguchi was a recipient of the IEEE ISSCC 2004 Takuo Sugano Outstanding Paper Award and the IEEE Kansai Section 2006 Gold Award. He has served as a Program Committee Member for IEEE Symposium on Low-Power and High-Speed Chips (COOL Chips), and as a Guest Associate Editor of IEICE Transactions on Fundamentals of Electronics, Communications and Computer Sciences. He is a member of the IEEE and ACM.